PAPER

Conversion of carbon dioxide in atmospheric pressure dielectric barrier discharges with different electrode configurations

Physica Scripta

PAPER

Conversion of carbon dioxide in atmospheric pressure dielectric barrier discharges with different electrode configurations

RECEIVED
20 April 2023

REVISED
18 June 2023

ACCEPTED FOR PUBLICATION
29 June 2023

PUBLISHED
14 July 2023

Chao Wang[1,2], **Hai-Xing Wang**[1,3,*], **Chang-Yu Liu**[1,2], **Xian Meng**[2,*], **Guang-Yuan Jin**[1], **He-Ji Huang**[2], **Jin-Wen Cao**[2], **Su-Rong Sun**[1,3] and **Cong Yan**[2]

[1] School of Astronautics, Beihang University, 102206, Beijing, People's Republic of China
[2] Institute of Mechanics, Chinese Academy of Sciences, Beijing 100190, Beijing, People's Republic of China
[3] Ningbo Institute of Technology, Beihang University, 315800, Ningbo, People's Republic of China
[*] Authors to whom any correspondence should be addressed.

E-mail: whx@buaa.edu.cn **and** mengxian@imech.ac.cn

Keywords: carbon dioxide decomposition, DBD, electrode configuration

Abstract

The choice of electrode configuration and dielectric material is critical to the discharge process and plasma characteristics of a dielectric barrier discharge (DBD) reactor. In this study, a new electrode configuration of DBD reactor with copper mesh as electrode inserted between dielectrics is proposed, which has a much higher capacitance than the conventional double-dielectric layer DBD reactor. Two materials with different relative dielectric permittivities, alumina and zirconia, are chosen as dielectrics for an experimental comparison of CO_2 decomposition. The experimental results show that the conversion rate of CO_2 for the reactor with copper mesh inserted between dielectrics are higher than that of the corresponding double dielectric layer reactor under the same discharge power, and the conversion rate of CO_2 with zirconia as a dielectric material is higher than the case of alumina as a dielectric. Further analysis of discharge characteristics shows that for the reactor with copper mesh inserted between dielectrics, the applied voltage required for discharge is significantly reduced, the amount of transferred charge is significantly increased, and the number of micro-discharge current pulses as well as the average lifetime during a single voltage cycle are also considerably increased, leading to an increase in the CO_2 discharge efficiency and conversion rate.

1. Introduction

Dielectric barrier discharges (DBD) under atmospheric pressure conditions themselves have the advantages of simple structure and moderate operating conditions and have a wide range of applications in a considerable number of industrial fields [1, 2]. The plasma formed by the dielectric barrier discharge has a distinctly non-equilibrium characteristic, where the temperature of heavy particles in the plasma system are close to room temperature and the electrons have relatively high energies, typically in the range of 1–10 eV, sufficient to break most chemical bonds, making it particularly suitable for the conversion, decomposition, and synthesis of compounds [3, 4]. DBDs are also well-scalable, robust and good-controllable plasma sources. Therefore, in recent years, the decomposition and conversion of carbon dioxide by means of DBD has received wide attention [5–7].

The efficient decomposition of CO_2 is difficult because of its high thermodynamic stability and the high energy required [8–13]. Previous studies on the chemical kinetics of CO_2 decomposition have shown that stepwise vibrational dissociation by electron impact is a more efficient solution than direct dissociation by electron impact, i.e., excitation of molecules of the lower vibrational energy levels of carbon dioxide by electron impact and gradual increase in the population density of molecules of the higher vibrational energy levels, which eventually leads to the dissociation of carbon dioxide molecules [10, 11, 14–18]. In contrast, a typical dielectric barrier discharge device is characterized by a relatively high reduced electric field, and the plasma system formed by the discharge has a high electron energy of about several eV. Therefore, in a DBD system, electron impact

dissociation of CO_2 ground state molecules dominates, and the corresponding conversion and energy efficiencies tend to be lower.

Therefore, from this aspect of DBD reactor, it is necessary to regulate the structure and operating parameters of the reactor to form suitable discharge conditions for the efficient conversion of CO_2. Previous extensive experimental studies on structural parameters of DBD reactors, such as dielectric thickness, discharge gap distance and length, and operating parameters such as applied voltage, frequency, power, gas flow rate, etc. have obtained a series of very informative results [6, 7, 19–22], which have greatly increased our knowledge and understanding of CO_2 decomposition in DBD reactors. As the key component of DBD reactor, the selection of dielectric materials has also gained wide attention. Quartz, alumina, zirconia, calcium oxide, and various ferroelectric materials have been tried as dielectric, dielectric coating, and even packing materials, the mechanism of plasma propagation in the dielectric packed bed reactors is investigated by experimental and numerical methods [23, 24], it is found that higher dielectric constants of packing material help to produce more intense, localized filamentary micro-discharges, and the experimental results show that different relative dielectric permittivities have certain effects on the conversion rate and energy efficiency of carbon dioxide [7, 20, 21, 25–28]. Under some conditions, it has been found that higher CO_2 conversion can be obtained by using materials with higher relative permittivity; however, under some conditions, it has been found that the CO_2 conversion does not necessarily increase with the increase of the relative permittivity of the materials. Further study found that the use of materials with higher relative permittivity would reduce the number of micro-discharge channels in the DBD reactor, increase the micro-discharge pulse current and make the discharge unstable, so the selection of dielectric material needs to be further combined with the reactor design to achieve the purpose of improving the CO_2 conversion [29].

Capacitance is a key parameter of DBD reactor and is a quantitative feature of the reactor electrode configuration, which largely determines the discharge current and other discharge characteristics of the reactor [1,22,30,31]. For example, in a recent study, the dielectric capacitance was modified by the means of the dielectric thickness in a plane to plane DBD configuration to investigate discharge homogeneity in air [32]. The capacitance of the reactor is not only related to the structural parameters of the reactor such as the gap distance, thickness of dielectric, but also to the dielectric material. Therefore, the main objective of this study is how to effectively combine the reactor design with the dielectric material to serve the purpose of improving the CO_2 conversion rate. We conducted a comparative experimental study on the decomposition of CO_2 in a double-layer dielectric reactor and a new reactor with a copper mesh inserted in the middle of the double-layer reactor as an electrode using different relative permittivities of dielectric materials (alumina or zirconia), and analyzed the effect of various parameters on the conversion rate by combining the discharge characteristics of the two reactors.

2. 2. Experimental setup

The experimental system used in this study and the structure of planar reactor are shown in figure 1. The discharge power of the DBD reactor is energized by a high voltage AC power supply (Nanjing Suman Plasma Technology Co., Ltd., CTP-2000K) with a maximum peak voltage of 30 kV. In the experiments, the output voltage frequency is set to 7 kHz at all conditions for comparison purposes. A high-voltage probe (Tektronix, P6015A) is used to measure the applied voltage of DBD reactor. An external resistor (50 Ω) and a capacitor (0.47 μF) are in series with DBD reactor to monitor the total current and transferred charge by a low voltage probe (Tektronix, P2220). All electrical signals are recorded by a four-channel digital oscilloscope (Tektronix, MDO3034). CO_2 (99.995% purity) is used as the feed gas with a flow rate of 10–50 sccm (standard cubic centimeters per minute) controlled by a mass flow controller (Beijing Sevenstar Electronics Co., Ltd., CS200-A). The discharge emission from the gas gap is collected and analyzed by a multi-channel spectrometer (Avantes, AvaSpec-ULS4096CL). After passing through the DBD reactor, the gas is analyzed by a gas chromatograph (Zhejiang Fuli, GC9790Plus) operating at atmospheric pressure. To evaluate the performance of plasma processing, the conversion of CO_2 is defined as follows

$$CO_2\ \text{conversion}(\%) = \frac{CO_2\ \text{converted}(\text{mol/s})}{CO_2\ \text{input}(\text{mol/s})} \times 100\% \quad (1)$$

The specific energy input (SEI) and energy efficiency (η) is defined to evaluate the energy cost of CO_2 decomposition

$$\text{SEI}(\text{kJ/L}) = \frac{\text{average discharge power}(\text{W})}{CO_2\ \text{flow rate (sccm)}} \times 60(\text{s/min}) \quad (2)$$

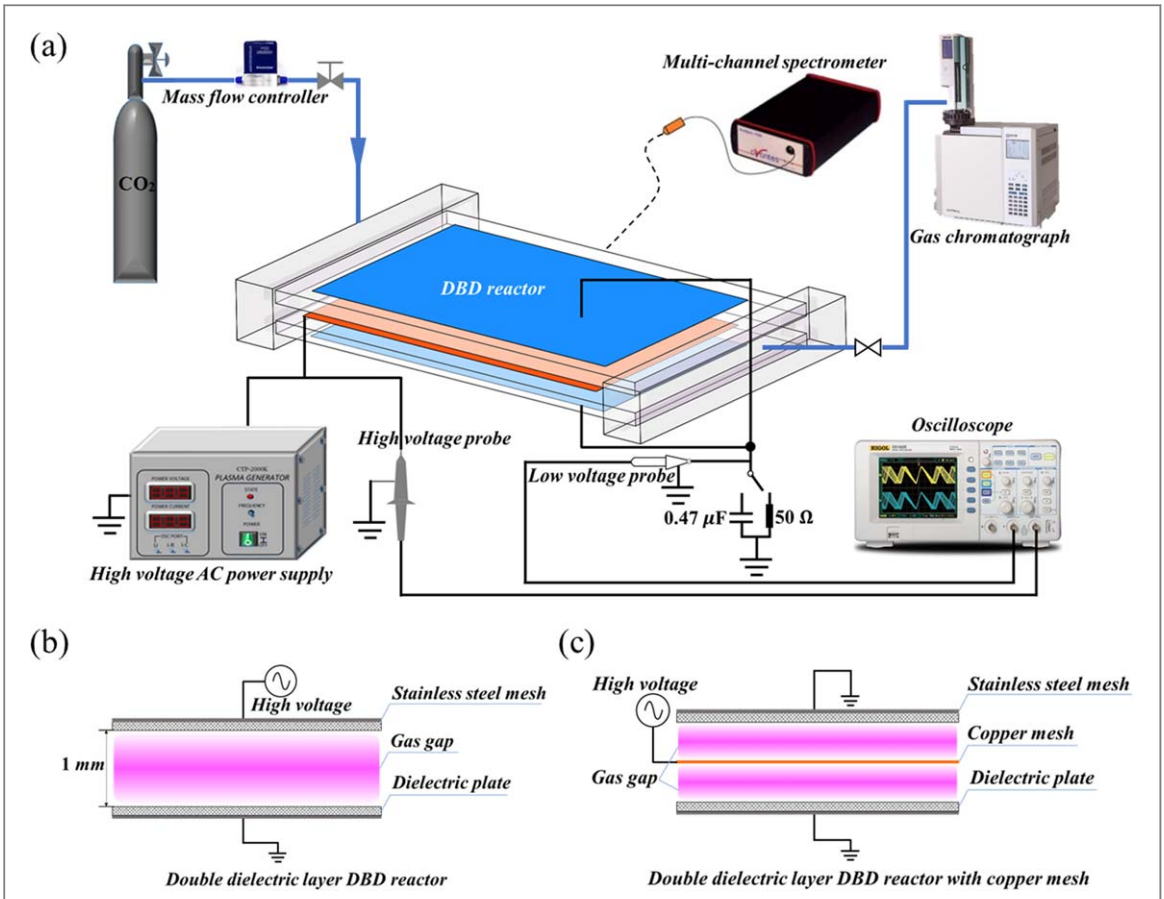

Figure 1. Schematic diagram of the (a) experimental setup, (b) double dielectric layer DBD reactor and (c) double dielectric layer DBD reactor with copper mesh.

$$\eta(\%) = \frac{\Delta \mathrm{H\ (kJ/mol)} \times \mathrm{CO_2\ conversion(\%)}}{22.4\mathrm{(L/mol)} \times \mathrm{SEI(kJ/L)}} \tag{3}$$

Here, ΔH represents the reaction enthalpy (283 kJ mol^{-1}) of pure CO_2 decomposition.

Two kinds of structure of the DBD planar reactors are used in the experiment as shown in figures 1(b) and (c). One structure is the conventional double dielectric planar reactor, using a length of 85 mm and width of 40 mm stainless steel mesh as electrodes. The thickness of the two dielectric plates is set to 2 mm and the discharge gap distance is set to 1 mm. The geometry of another DBD reactor is the same as the main body of the double dielectric layer reactor, the main difference is that a piece of copper mesh (400 mesh) with dimensions of 85 mm length and 40 mm width is inserted in the middle of double dielectric layer reactor as a high voltage electrode, and the electrodes on the other side of the dielectric are grounded. In this case, the gap on both sides of the copper mesh electrode is 0.5 mm, respectively. The dielectric materials used in the experiment are alumina and zirconia, respectively.

For double dielectric layer planar reactor, the geometrically determined dielectric capacitance C_{diel} can be calculated according to the following equation

$$C_{diel} = \frac{\varepsilon_0 \varepsilon_r S}{d} \tag{4}$$

here, S is the opposite area between the two planar electrodes, d is the thickness of the dielectric barrier, ε_0 represents the vacuum permittivity and ε_r represents the relative permittivity of dielectric. The insertion of a copper mesh in a double dielectric reactor with the same spacing corresponds to a parallel connection of two metal electrode-single dielectric reactors. Therefore, compared with the double dielectric reactor without copper mesh, the dielectric thickness and surface area of the double dielectric reactor with copper mesh become $1/2d$ and $2S$, respectively, so that its dielectric capacitance is equal to 4 times that of the double dielectric reactor without copper mesh.

This method of combining the electrode setup with the relative permittivity of the materials allows us to design DBD reactors with different capacitances, and the reactor dielectric capacitance C_{diel} obtained in this study using two kinds of dielectric materials alumina and zirconia in combination with the electrode setup is given in table 1. In the subsequent experiments, we then used four reactors with different capacitances

Table 1. Physical properties of the two dielectric materials and dielectric capacitances of reactors.

Dielectric material	Chemical composition	Relative permittivity (ε_r)	Dielectric capacitance of double layer reactor (pF)	Dielectric capacitance of double layer reactor with copper mesh (pF)
Alumina	Al_2O_3 99.70% Na_2O 0.15% SiO_2 0.10%	9.6	72	288
Zirconia	ZrO_2 96.5% MgO 0.51% CaO 0.10%	25	188	752

Table 2. Comparison of dielectric capacitances for the coaxial DBD reactor and the double dielectric layer DBD reactor with a copper mesh.

Dielectric material	Relative permittivity (ε_r)	Dielectric capacitance of the coaxial DBD reactor (pF)	Dielectric capacitance of double layer reactor with copper mesh (pF)
Alumina	9.6	120	288
Zirconia	25	313	752

composed of different dielectric materials and different electrode configurations to investigate their effects on the CO_2 conversion performance.

It is worth noting that a coaxial DBD reactor which contains a central electrode rod and a copper mesh on the outside of a dielectric tube is widely used in most experimental research works about CO_2 decomposition by atmospheric pressure DBD [3, 4, 19, 21, 22, 26–28, 33]. The comparison between the double dielectric layer DBD reactor with a copper mesh and a coaxial DBD reactor is helpful to deepen the understanding of the influence of the structural characteristics of the two reactors on CO_2 decomposition performance.

Under the premise of the same gas gap distance, dielectric layer thickness and outer electrode area, a coaxial DBD reactor and the double dielectric layer DBD reactor with a copper mesh may have the following three differences. First, the capacitance of the coaxial DBD reactor is different from that of the double dielectric layer DBD reactor with a copper mesh. The coaxial DBD reactor is equivalent to an asymmetric capacitor while the double dielectric layer DBD reactor with a copper mesh is equivalent to a symmetric capacitor. As a result, the dielectric capacitance and reactor capacitance of the two DBD reactors are different from each other. Here, the dielectric capacitance of the coaxial DBD reactor is calculated according to the following equation [33]

$$C_{\text{diel}} = \frac{2\pi\varepsilon_0\varepsilon_r l}{\ln\left((d+x)/d\right)} \tag{5}$$

where l is the length of the outer copper mesh, d and x are the inner diameter and thickness of the dielectric tube, respectively. The calculation results for the coaxial DBD reactor are given in table 2 and compared to the dielectric capacitance of double dielectric layer DBD reactor with a copper mesh.

As can be seen from table 2, the dielectric capacitance of the coaxial DBD reactor is lower than that of the double dielectric layer DBD reactor with a copper mesh, which indicates that the double dielectric layer DBD reactor with a copper mesh has a better ability to store electrical charge than the coaxial DBD reactor. This could be beneficial for CO_2 decomposition.

Secondly, the electric field distribution inside the two DBD reactors with different structures is different. For the double dielectric layer DBD reactor with a copper mesh, the electric field in the reactor is a uniformly distributed electric field in the absence of discharge. However, the electric field in the coaxial DBD reactor shows a radial distribution and it is a non-uniform electric field. Typical electric field strength distribution inside a coaxial DBD reactor can be found in figure 3(a) of [34]. It is expected that the non-uniform distribution of electric field in the coaxial DBD reactor could affect the CO_2 decomposition to some extent.

Finally, in this double dielectric layer DBD reactor with a copper mesh, the copper mesh is directly exposed to the plasma. The copper mesh of the coaxial DBD reactor is located on the outside of a dielectric tube, and its central electrode rod is directly exposed to the plasma instead of the copper mesh. As reported in [22], the surface structure of electrode has a considerable effect on the discharge characteristic and CO_2 decomposition performance of a DBD reactor. The metal mesh electrode directly exposed to plasma in a DBD reactor helps to enhance the amplitude and number of current pulses as well as the transferred charge, which can further improve the CO_2 decomposition performance of a DBD reactor.

Figure 2 shows a typical example of the Q-V plot of the DBD, which is also known as the Lissajous figure, and the equivalent circuit of a DBD reactor. In figure 2(a), the lines AB and CD represent the period of discharge-off in the DBD reactor when only displacement currents are present. The slope of these two lines corresponds to the

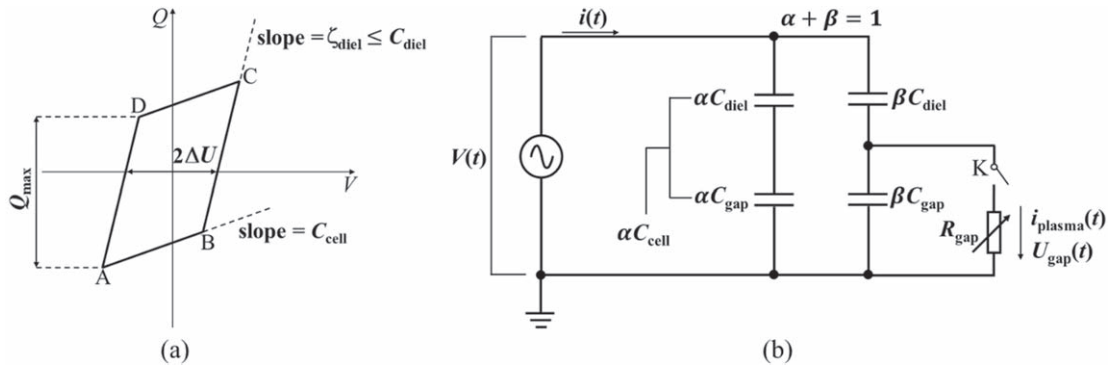

Figure 2. (a) A typical Q–V plot of the DBD and (b) equivalent circuit of a DBD reactor.

total capacitance of DBD reactor C_{cell} without plasma discharge, which is composed of the dielectric capacitance C_{diel} and the gap capacitance C_{gap}. Lines AD and BC represent the discharge-on phase when the gas breakdown occurs in the gap and plasma is ignited. The slope of these lines is the effective dielectric capacitance ζ_{diel} and should be equal to C_{diel} for a fully discharge bridged gap [31, 35, 36].

Under atmospheric pressure conditions, molecular gas discharges in DBD reactor gaps usually operate in filamentary discharge mode, which is characterized by the presence of a large number of narrow micro-discharge channels with very short lifetimes (1–10 ns), and the micro-discharge channels are randomly distributed throughout the discharge volume [1, 37]. Therefore, for filamentary discharge mode, the discharge within the DBD reactor gap is not uniform and the charge on the dielectric surface may not be completely transferred and is a case of partial surface discharging, and then the discharge usually does not cover the entire available electrode area [38–40]. Considering this inhomogeneity of the discharge in the planar DBD reactor, the original simple circuit model based on the lumped parameter method should be further modified to more reasonably evaluate the electrical characterization of the discharge process [37]. Based on this consideration, Peeters *et al* proposed an alternative equivalent circuit model, as shown in figure 2(b) [38]. In this model, the electrode area of the planar reactor is divided into non-discharging and discharging area components with fractions α and β, respectively. The actual measured slope of AD and BC in Q-V plot, called the effective dielectric capacitance ζ_{diel}, which is a linear combination of the total capacitance of the reactor C_{cell}, and the dielectric capacitance C_{diel}.

Based on the Q-V plots obtained from experimental measurements, the maximum charge transferred through the gas gap Q_{max}, the effective dielectric capacitance ζ_{diel}, the equivalent total capacitance of the reactor C_{cell} and the intercept ΔU on the horizontal axis of the side with the larger slope of the Q-V plot can be obtained. Combined with the experimentally collected physical quantities (applied voltage $V(t)$ of DBD reactor, total circuit current $i(t)$, and total transferred charge $Q(t)$ of the circuit), the discharge gap voltage $U_{gap}(t)$ and plasma conduction current $i_{plasma}(t)$ can be calculated as follows

$$U_{gap}(t) = \left(1 + \frac{\alpha}{\beta}\frac{C_{cell}}{C_{diel}}\right)V(t) - \frac{Q(t)}{\beta C_{diel}} \tag{6}$$

$$i_{plasma}(t) = \frac{1}{1 - C_{cell}/C_{diel}}\left[i(t) - C_{cell}\frac{dV(t)}{dt}\right] \tag{7}$$

The physical quantities such as the conductively transferred charge during the discharge per half-cycle ΔQ_{dis}, the equivalent gap capacitance C_{gap}, the non-discharging area fraction α, the discharging area fraction β, and the voltage across the gas gap during the discharge, U_b, referred to as the burning voltage can be calculated based on this equivalent circuit model of DBD [38], which can be used to further analyze the discharge characteristics under different electrode configurations.

3. Results and discussions

3.1. Effect of electrode configuration and dielectric materials on CO_2 conversion and energy efficiency

As mentioned above, capacitance characterizes the ability of a device or equipment to store electrical charge. Capacitance is related to both the geometry of the reactor design, e.g., the relative surface area of the dielectric plates and the distance between them, and the relative dielectric permittivity of the dielectric material. A combination of two different dielectric materials and two different configurations of electrodes can be

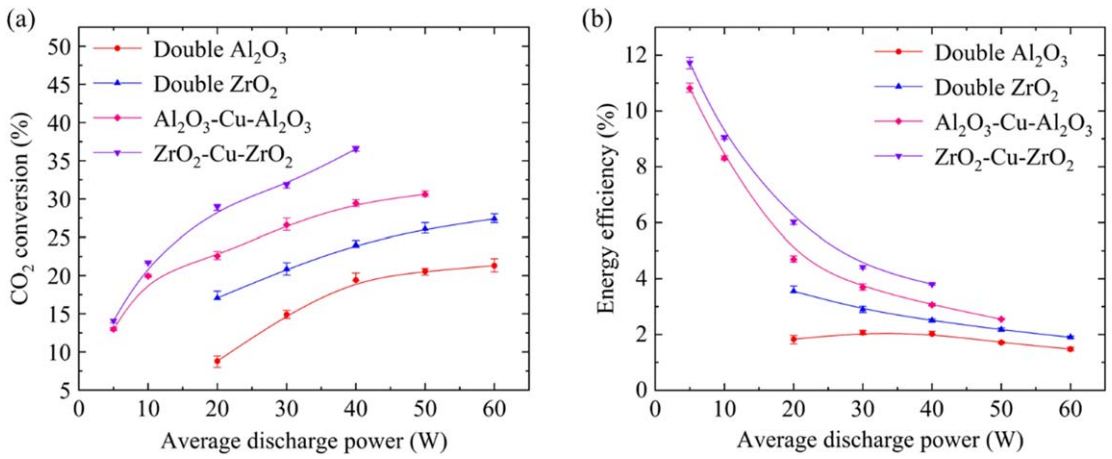

Figure 3. (a) CO_2 conversion rate and (b) energy efficiency as a function of discharge power for DBD reactors with different electrode configurations (CO_2 flow rate of 20 sccm).

considered to adjust the capacitance of the reactor to some extent. Under the condition of atmospheric pressure DBD, the main products of CO_2 decomposition are carbon monoxide and oxygen [26]. A comparison of the conversion rate and energy efficiency obtained for the decomposition of CO_2 in a double dielectric layer reactor with alumina or zirconia plates as dielectric layers, respectively (identified in the figure as Double Al_2O_3, and Double ZrO_2) and in a double dielectric reactor with copper mesh electrode inserted between the corresponding double dielectric layers (identified in the figure as Al_2O_3-Cu-Al_2O_3 and ZrO_2-Cu-ZrO_2) is presented in figure 3.

As can be seen from figure 3(a), firstly, corresponding to the same reactor structure, the reactor composed of ZrO_2 with a larger relative permittivity presents a higher CO_2 conversion rate than that of the Al_2O_3 reactor with a smaller relative permittivity. Secondly, the CO_2 conversion rates of the double-dielectric layer reactor with copper mesh are much higher than those of the double-dielectric layer reactor without copper mesh. Among them, for the ZrO_2-Cu-ZrO_2 reactor, the CO_2 conversion is as high as 36% at a discharge power of 40 W and a CO_2 flow rate of 20 sccm. The energy efficiency of CO_2 conversion corresponding to different discharge powers is given in figure 3(b). In general, the energy efficiency decreases with increasing discharge power, and the energy efficiencies of the double-dielectric layer reactor with a copper mesh electrode are higher and can reach more than 10% at lower power levels.

It is noteworthy that for the reactor with the same electrode configuration and the same geometry, the reactor capacitance is only related to the relative permittivity of the material. With the increase of relative permittivity of the dielectric, the reactor capacitance increases. For double dielectric layer reactors with or without copper mesh electrode, the change of electrode configuration also leads to the change of reactor capacitance. For the double-dielectric layer reactor with copper mesh in the middle, its reactor capacitance is larger than that of double dielectric layer reactor without copper mesh electrode. According to the above trends of the conversion rate and energy efficiency changes of CO_2 decomposition for reactors with different electrode configurations, it is clear that increasing the reactor capacitance helps to improve the conversion rate and energy efficiency of CO_2 decomposition.

The variation of CO_2 conversion and energy efficiency with CO_2 flow rate for different electrode configurations is given in figure 4. It is seen from the figure that the CO_2 conversion and energy efficiency follow a similar trend for different configurations, with the CO_2 conversion increasing and the energy efficiency decreasing as the CO_2 flow rate decreases. Over the entire gas flow variation range, the conversion rates and energy efficiencies of the reactor composed of dielectric material with higher relative permittivity are higher than that of the low relative permittivity case. The performance of the double-dielectric layer reactor with copper mesh electrode is better than that of the double-dielectric layer reactor without copper mesh electrode. For the ZrO_2-Cu-ZrO_2 reactor, the CO_2 conversion is higher than 40% at a discharge power of 40 W and a CO_2 flow rate of 10 sccm.

3.2. Effect of electrode configuration and dielectric material on the electrical characteristic of a DBD reactor

As mentioned above, the *Q*-*V* plot, *i.e.*, the Lissajous figure, contains important information about the DBD reactor. Figure 5 shows the *Q*-*V* curves for the decomposition of CO_2 in a DBD reactor with different electrode configurations. It is seen that the corresponding *Q*-*V* curves of different reactors vary greatly, with the Al_2O_3-Al_2O_3 reactor having the highest applied voltage amplitude and the lowest transferred charge, and the ZrO_2-Cu-ZrO_2 reactor having the lowest applied voltage amplitude and the highest transferred charge. Based on

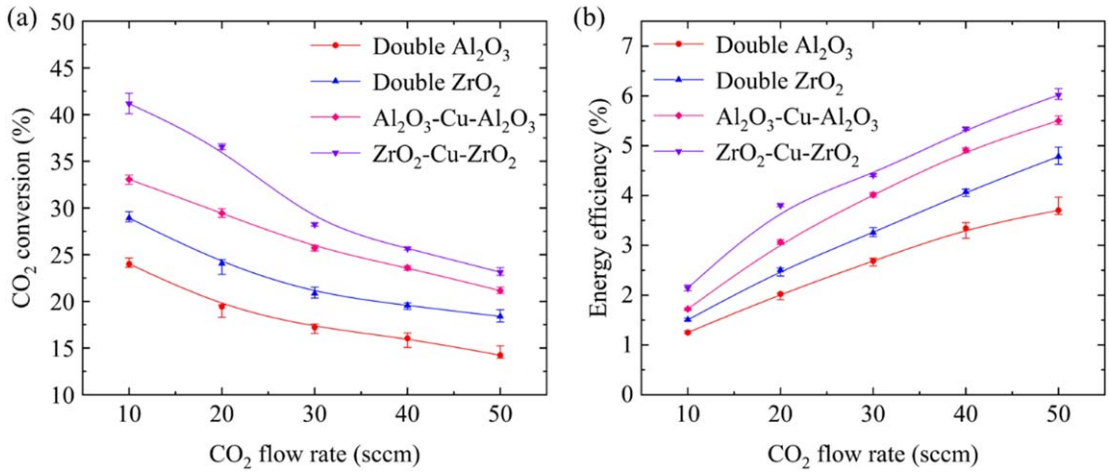

Figure 4. (a) CO_2 conversion rate and (b) energy efficiency as a function of CO_2 flow rate for DBD reactors with different electrode configurations (discharge power of 40 W).

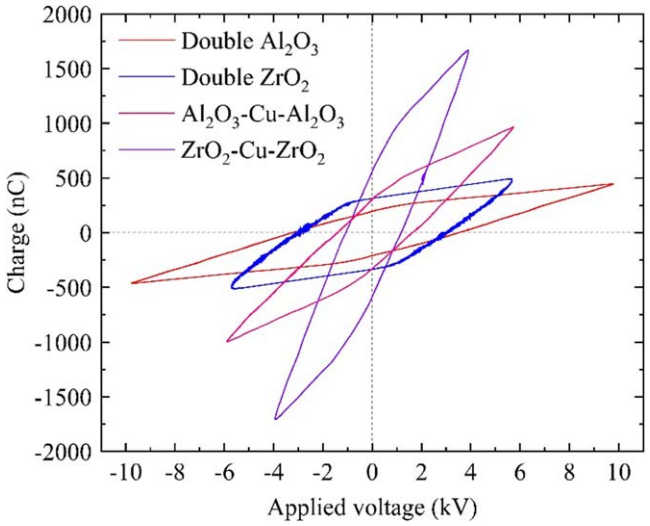

Figure 5. *Q-V* plots measured for DBD reactors with different electrode configurations (discharge power of 40 W, CO_2 flow rate of 20 sccm).

figure 5 and the previous equivalent circuit model considering the case of partial surface discharging, the reactor capacitance C_{cell} as well as the effective dielectric capacitance ζ_{diel} can be obtained, as shown in figure 6. According to the previous discussion, it is known that the reactor capacitance C_{cell} reflects the characteristics of the electrode configuration during the discharge-off period of a DBD reactor.

As can be seen in figure 6(a), for the ZrO_2-Cu-ZrO_2 reactor, the C_{cell} value is more than twice that of the Al_2O_3-Cu-Al_2O_3 reactor and more than five times higher than that of the ZrO_2-ZrO_2 or Al_2O_3-Al_2O_3 reactor without copper mesh electrode. Although the double dielectric layer reactor also shows the higher dielectric permittivity, the larger reactor capacitance value C_{cell}, the use of double dielectric layer with copper mesh configuration has a more obvious effect on the capacitance value of the reactor. From the effective dielectric capacitance values ζ_{diel} given in figure 6(b) for the active discharge phase, it appears that for all the reactors with different electrode configurations, the ζ_{diel} values for the ZrO_2-Cu-ZrO_2 reactor are much higher than the other reactors. The ζ_{diel} values increase with the increase of the discharge power. The main reason for this is that more micro-discharge channels are formed and more charges are transferred between the electrodes as the discharge power increases. As a result, the ζ_{diel} values become closer and closer to the geometrically determined dielectric capacitance C_{diel}.

The conversion of CO_2 in the DBD can be described as a function of the total number of charges transferred by the gas during its residence time in the active plasma region [41]. Therefore, the transferred charge derived from the *Q-V* curves measured is also an important indicator of the discharge characteristics of the DBD reactor

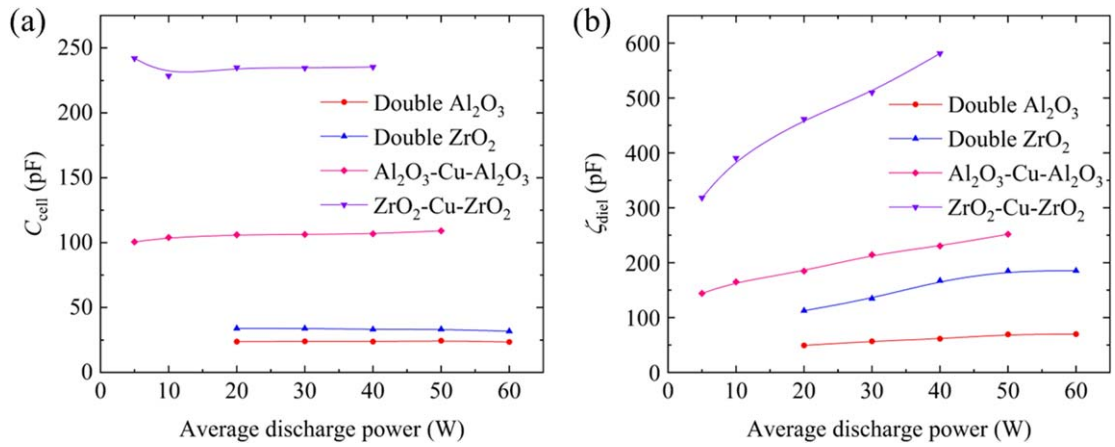

Figure 6. (a) The cell capacitance, (b) effective dielectric capacitance as a function of discharge power extracted from the Q–V plots for DBD reactors with different electrode configurations (CO_2 flow rate of 20 sccm).

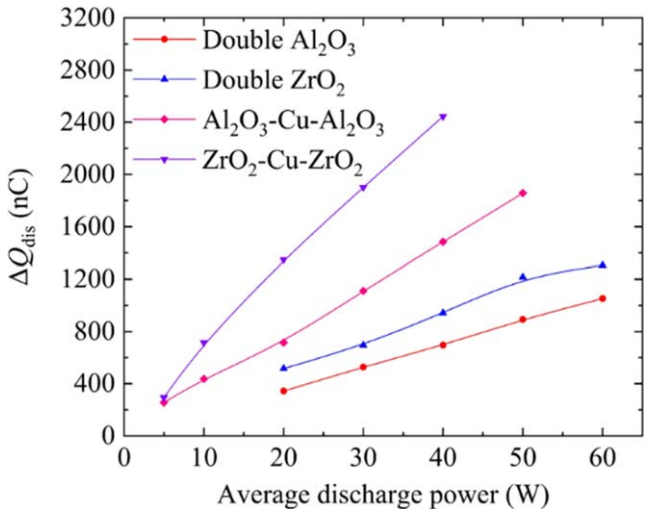

Figure 7. Variation of the conductively transferred charge during the discharge per half-cycle with discharge power for DBD reactors with different electrode configurations (CO_2 flow rate of 20 sccm).

with different electrode configurations. One the one hand, the amount of charge transferred in the reactor is related to the nature of the gas, so the more charge transferred during the discharge process indicates the higher electron number density in the discharge system and the more reactive the gas is, thus favoring the conversion of CO_2. On the other hand, the amount of transferred charge is related to the size of the reactor geometry and the relative permittivity of dielectric.

From figure 7, it is seen that the reactor with ZrO_2 as dielectric has a higher charge transfer capacity than the Al_2O_3 reactor, and the reactor with copper mesh electrode has a higher charge transfer capacity than the reactor without copper mesh electrode. The conductively transferred charge increases almost linearly as the discharge power increases. For ZrO_2-Cu-ZrO_2 reactor, the maximum conductively transferred charge per half-cycle can reach more than 2400 nC. This indicates that the use of high relative permittivity materials and reasonable electrode configurations can significantly improve the charge transfer capacity of DBD reactor.

Note that the discharge power range is different for the double dielectric layer DBD reactor and the double dielectric layer DBD reactor with a copper mesh in figure 3. The discharge power range of a DBD reactor is related to its structure, dielectric material and many other factors. On the one hand, the double dielectric layer DBD reactor requires a higher applied voltage to maintain the discharge, as shown in figure 5. Under low discharge power conditions (such as 5 W, 10 W), the gap voltage of the double dielectric layer DBD reactor is so low that CO_2 gas cannot be broken down and a stable discharge cannot be maintained. However, for the double dielectric layer DBD reactor with a copper mesh, the insertion of copper mesh electrode effectively halves the gas gap distance and enhances the ability of a DBD reactor to transfer charge, which results in a lower applied voltage

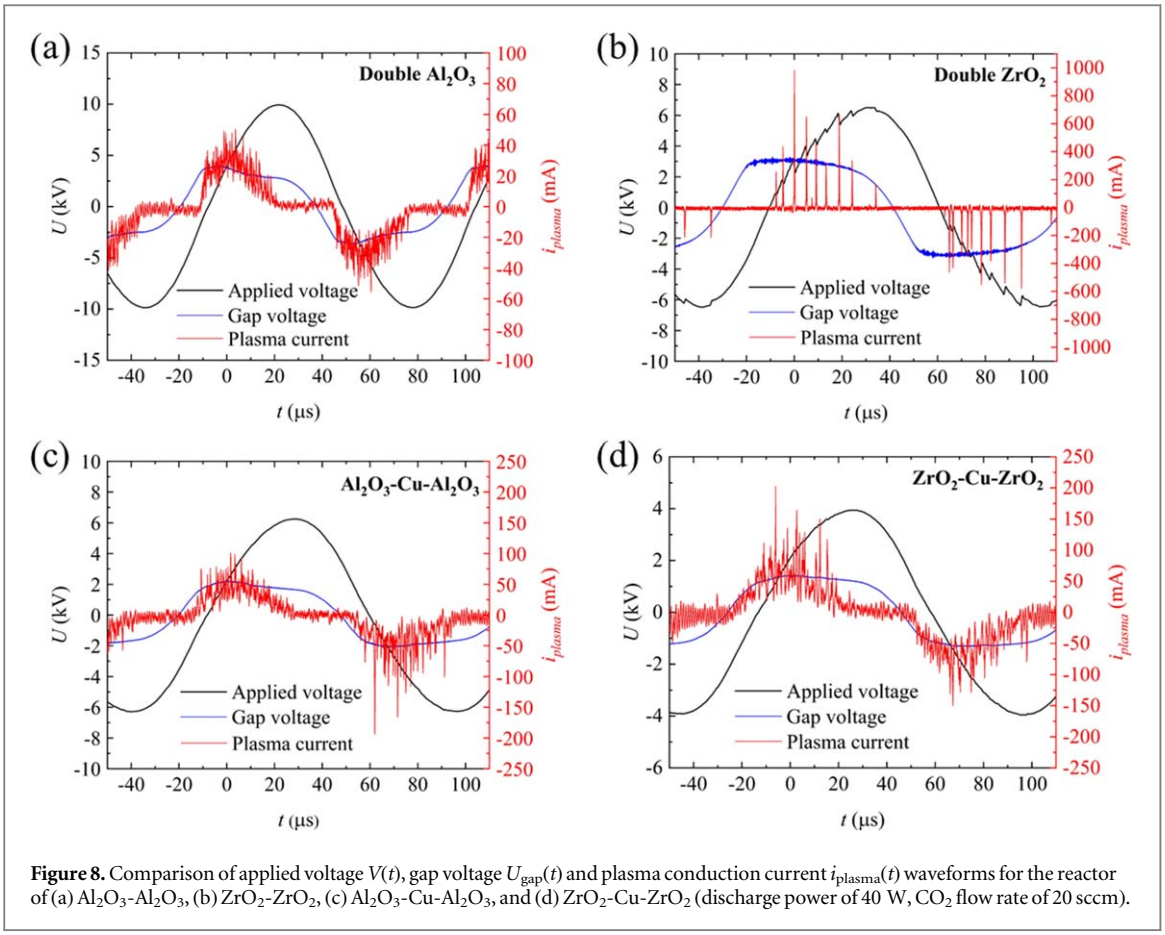

Figure 8. Comparison of applied voltage $V(t)$, gap voltage $U_{gap}(t)$ and plasma conduction current $i_{plasma}(t)$ waveforms for the reactor of (a) Al_2O_3-Al_2O_3, (b) ZrO_2-ZrO_2, (c) Al_2O_3-Cu-Al_2O_3, and (d) ZrO_2-Cu-ZrO_2 (discharge power of 40 W, CO_2 flow rate of 20 sccm).

and allows a DBD reactor to operate under lower discharge power conditions (5 W, 10 W). On the other hand, when the discharge power is high enough, the filamentary discharge in a DBD reactor is easy to transition to an arc discharge. The average current intensity of the double dielectric layer DBD reactor with a copper mesh is higher than that of the double dielectric layer DBD reactor under the same discharge power condition. When the discharge power rises, the filamentary discharge in the double dielectric layer DBD reactor with a copper mesh is more likely to transition to an arc discharge, so the maximum discharge power of the double dielectric layer DBD reactor with a copper mesh is lower than that of the double dielectric layer DBD reactor.

3.3. Effect of electrode configuration and dielectric material on the micro-discharge characteristic of a DBD reactor

The applied voltage of DBD reactor $V(t)$, gap voltage $U_{gap}(t)$, and plasma conduction current $i_{plasma}(t)$ waveforms can provide rich information for studying the micro-discharge characteristics of DBD reactors. In figure 8, the black line indicates the applied voltage of DBD reactor, the red line indicates the conduction current through the discharge gap obtained from the calculation of equation (7), and the blue line indicates the gap voltage obtained from the calculation of equation (6). As can be seen from the conduction current waveforms of the different electrode configurations of DBD reactors given in figure 8, the discharge is characterized by multiple current pulses per half-cycle, and the duration of these current pulses is extremely short, typically less than one microsecond. The presence of multiple short-lived current pulses per half-cycle is usually considered as a sign of filamentary discharge established in the gap between the dielectric layers.

From figure 8, it can be found that the applied voltage amplitudes of DBD reactors with different electrode configurations are different. The reactor with copper mesh electrode has a lower applied voltage than the reactor without copper mesh electrode. Similarly, the gap voltage during the active discharge phase of the reactor with copper mesh electrode is lower than that of the reactor without copper mesh electrode. It can be seen that the presence of multiple current pulses in the reactors has a good synchronization with the gap voltage, that is, when the gap voltage reaches a certain threshold, a large number of discharge current pulses start to appear, then the gap voltage seems to enter a plateau area with less variation [19, 38]. From the comparison of four different electrode configurations, it can be seen that the voltage range of the DBD reactor composed of different dielectric materials, the number of current pulse peaks varies greatly, which is a comprehensive reflection of the interaction between the reactor electrode configurations and the discharge characteristics of carbon dioxide

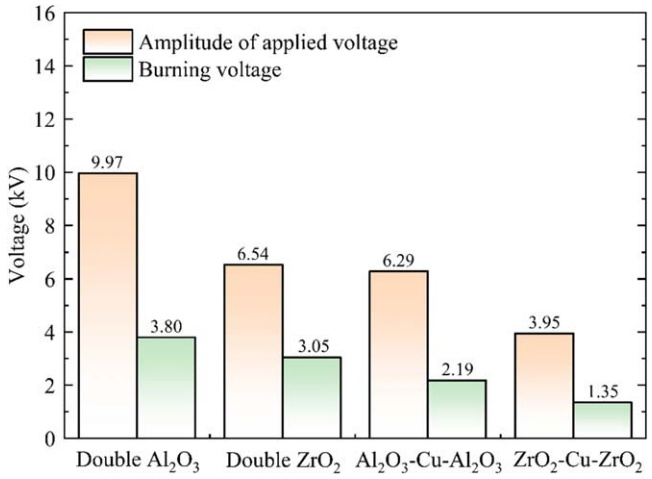

Figure 9. Comparison of applied voltage amplitude and burning voltage for DBD reactors with different electrode configurations (discharge power of 40 W, CO_2 flow rate of 20 sccm).

Table 3. Comparison of the electrical parameters for the double dielectric layer DBD reactor without copper mesh and the double dielectric layer DBD reactor with a copper mesh (average discharge power of 50 W, CO_2 flow rate of 20 sccm).

DBD reactor	C_{diel} (pF)	ζ_{diel} (pF)	C_{cell} (pF)	ΔQ_{dis} (nC)	U_b (kV)	E (kV/cm)
Double Al_2O_3 (gap 0.5 mm)	72	71.0	37.2	1171	2.32	46.4
Al_2O_3-Cu-Al_2O_3	288	252	109	1857	2.14	42.9

itself. Further analysis of the connection between the two aspects can provide a reference for further improvement of the reactor design to enhance the performance of CO_2 decomposition and conversion.

Figure 9 shows the comparison of the applied voltage amplitude extracted from applied voltage waveforms given in figure 8 and the burning voltage calculated based on the Q-V plots given in figure 5. It can be seen from figure 9 that the applied voltage amplitude decreases from 9.97 kV for the Al_2O_3-Al_2O_3 reactor to 3.95 kV for the ZrO_2-Cu-ZrO_2 reactor, while the burning voltage reduces from 3.80 kV for the Al_2O_3-Al_2O_3 reactor to 1.35 kV for the ZrO_2-Cu-ZrO_2 reactor. Under the same electrode configuration, the use of dielectric materials with higher relative permittivity can significantly reduce the values of applied voltage amplitude and burning voltage. This is because the burning voltage of DBD is largely influenced by the surface charge density generated by the previous discharge with AC power, which depends on the capacitance of the dielectric [42]. The larger the relative permittivity of the dielectric material, the higher its capacitance value, so that the reactor with ZrO_2 as dielectric barriers corresponds to a lower burning voltage than the reactor with Al_2O_3 as dielectric barriers. There are two main reasons for the further reduction of the burning voltage for the reactor with a copper mesh electrode, firstly because of the shortening of the gap distance between the electrodes due to the copper mesh as an electrode, and secondly because the copper mesh as an electrode helps to enhance the charge transfer process.

As mentioned above, the insertion of a copper mesh into a double dielectric layer DBD reactor is equivalent to a parallel connection of two metal electrode-single dielectric DBD reactors, and the gas gap distance between the copper mesh electrode and the dielectric plate is 0.5 mm. The role of the copper mesh electrode can be further elucidated by comparing the CO_2 decomposition performance of the double dielectric layer DBD reactor with a gas gap distance of 0.5 mm to that of the double dielectric layer DBD reactor with a copper mesh. It is worth noting that although the gas gap distance of the two DBD reactors is the same, the electrical characteristics of them are inconsistent. Because the double dielectric layer DBD reactor without copper mesh has two dielectric layers between its high voltage electrode and ground electrode, while the double dielectric layer DBD reactor with a copper mesh is equivalent to a parallel connection of two metal electrode-single dielectric DBD reactors and there is only one dielectric layer between its high voltage electrode and ground electrode. In the comparison experiment, the average discharge powers of the two DBD reactors are 50 W, respectively. The CO_2 flow rate changes from 10 sccm to 50 sccm. The alumina is used as dielectric barrier here.

Table 3 presents all the electrical parameters of the two DBD reactors at a discharge power of 50 W and a CO_2 flow rate of 20 sccm (The double dielectric layer DBD reactor without copper mesh is denoted as 'Double Al_2O_3 (gap 0.5 mm)', and the double dielectric layer DBD reactor with a copper mesh is denoted as 'Al_2O_3-Cu-Al_2O_3'). The geometrically determined dielectric capacitance C_{diel}, effective dielectric capacitance ζ_{diel}, cell capacitance

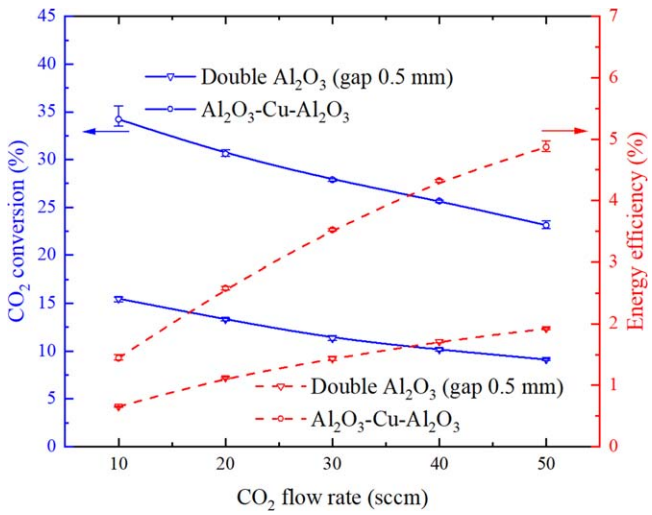

Figure 10. CO_2 conversion and energy efficiency as a function of CO_2 flow rate for the double dielectric layer DBD reactor without copper mesh and the double dielectric layer DBD reactor with a copper mesh (average discharge power of 50 W).

C_{cell}, conductively transferred charge during the discharge per half-cycle ΔQ_{dis}, and burning voltage U_b of the two DBD reactors shown in table 3 are calculated according to the methods mentioned in section 2. The average electric field strength E during the discharge is also determined by the ratio of burning voltage to the gas gap distance [43].

As can be seen from table 3, the double dielectric layer DBD reactor without copper mesh has a lower effective dielectric capacitance and cell capacitance than the double dielectric layer DBD reactor with a copper mesh. In addition, the conductively transferred charge per half-cycle of the double dielectric layer DBD reactor without copper mesh is also much lower than that of the double dielectric layer DBD reactor with a copper mesh. The electric field strength in the double dielectric layer DBD reactor without copper mesh is higher than that of the double dielectric layer DBD reactor with a copper mesh.

Figure 10 shows the CO_2 decomposition performance of the two DBD reactors. It is seen that the CO_2 conversion and energy efficiency of the double dielectric layer DBD reactor without copper mesh are both much lower than those of the double dielectric layer DBD reactor with a copper mesh under all CO_2 flow rate conditions. Combined with the discharge characteristic parameters presented in table 3, it appears that in this situation, the increase of electric field strength is not enough to improve CO_2 conversion and energy efficiency without the copper mesh.

A large number of micro-discharge processes formed in the dielectric barrier discharge gap are actually the response of the CO_2 system to the instantaneous energy input [44], influenced by the amount of charge stored on the dielectric surface as well as the surface morphological properties, thus showing a random spatial-temporal distribution. By observing and analyzing the basic characteristics of micro-discharge, the modulation effect of different electrode configurations and dielectric materials on the discharge process and the influence on the characteristics of micro-discharge can be summarized and analyzed. Using a method similar to [19], the main parameters describing the characteristics of the micro-discharge process, such as the number of micro-discharge current pulses per cycle N_{md}, the average value of micro-discharge current pulses, and the average lifetime of micro-discharge current pulses can be analyzed according to the conduction current waveforms of reactors with different electrode configurations given in figure 8. It is worth pointing out that the micro-discharge characteristics obtained here do not represent real physical individual micro-discharge channel, but the actual combined characteristics of a large number of micro-discharge channels in the discharge gap at a given moment.

As can be seen from figure 11(a), for the double-dielectric layer reactor, the number of micro-discharge current pulses for Al_2O_3-Al_2O_3 reactor is much higher than that of ZrO_2-ZrO_2 reactor. This difference in the number of current peaks can also be seen from the conduction current waveforms in figure 8, and the reason for this phenomenon may be strongly related to the surface morphological characteristics of the two dielectrics. It can also be seen from figure 11(a) that the number of micro-discharge peaks in both double-dielectric layer reactors without copper mesh electrode is smaller than that in double-dielectric layer reactors with copper mesh electrode. For the double-dielectric layer reactors with copper mesh electrode, which is composed of two different dielectrics, the corresponding number of micro-discharge peaks are very close to each other, indicating that the use of copper mesh as the electrode can significantly improve the micro-discharge characteristics in the reactor, increase the number of micro-discharge peaks, and improve the uniformity of discharge in the gas gap.

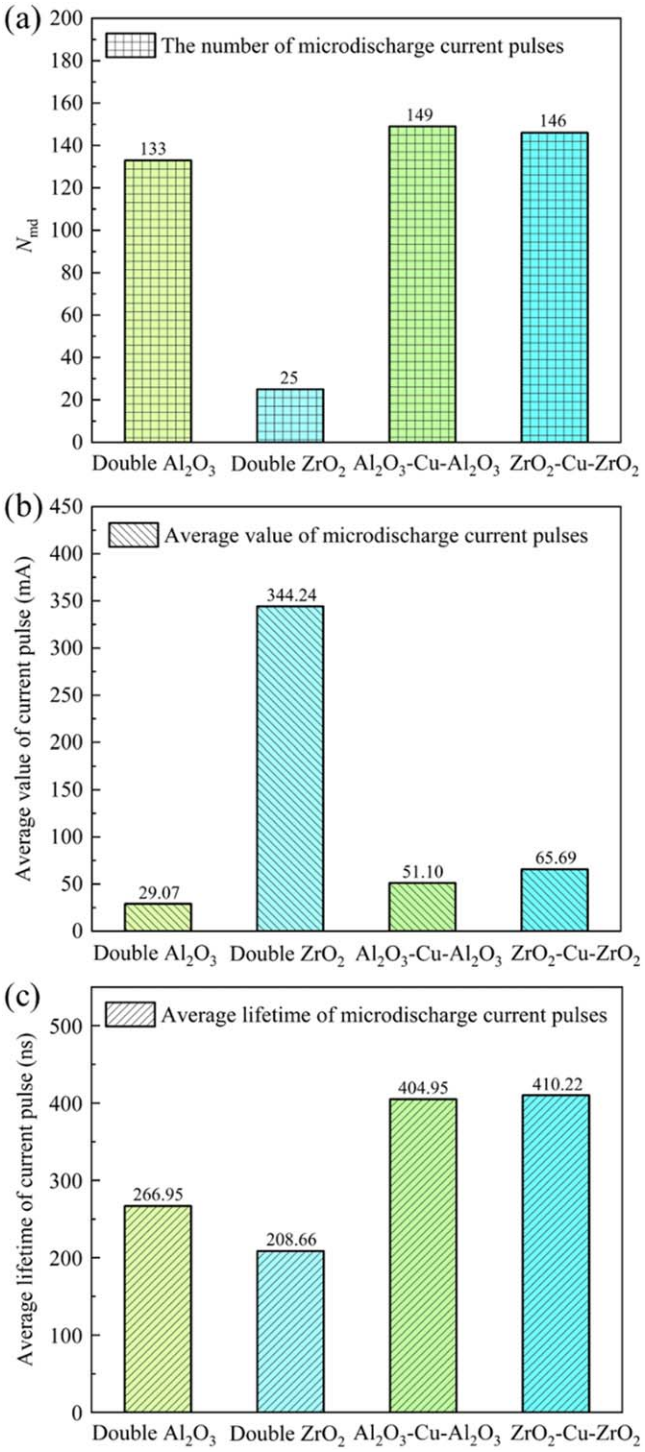

Figure 11. (a) Number of micro-discharge current pulses per cycle, (b) average current intensity and (c) average lifetime of micro-discharge current pulses per cycle for DBD reactors with different electrode configurations (discharge power of 40 W, CO_2 flow rate of 20 sccm).

The average values of micro-discharge current pulses for the reactors with different electrode configurations are given in figure 11(b), from which it is seen that the average values of current pulses for the double-layer zirconia reactor are much higher than the other cases. The main reason needs to be analyzed in conjunction with the conductively transferred charge shown in figure 7 and the number of micro-discharge peaks in figure 11 (a). For the ZrO_2-ZrO_2 reactor, the amount of conductively transferred charges during discharge is larger, but the number of micro-discharge peaks is lower, resulting in a larger average value of the current pulse. The large pulse current intensity of micro-discharge will cause the discharge to be unstable and it is possible for the DBD to evolve into arc discharge, which is not conducive to the long-term operation of the reactor. It can also be seen from figure 11 that for the double dielectric reactor with copper mesh electrode, the amount of conductively

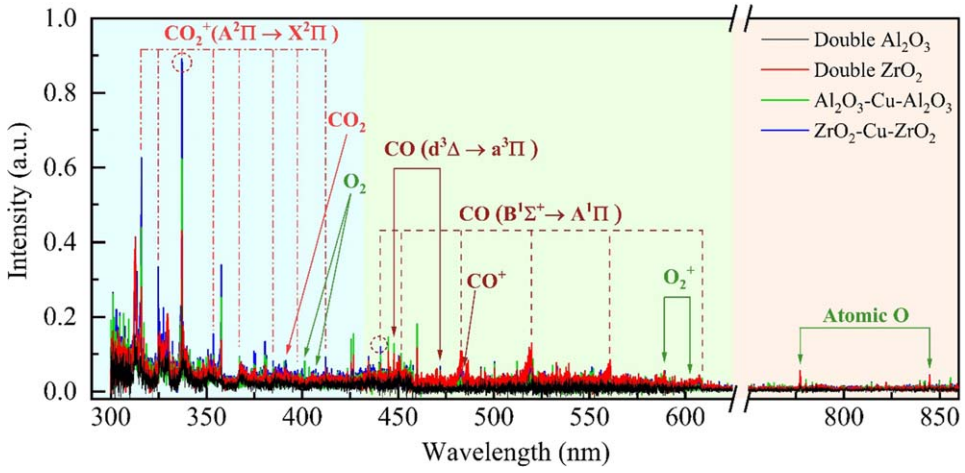

Figure 12. Optical emission spectra of the CO_2 discharge in different DBD reactors (discharge power of 40 W, CO_2 flow rate of 20 sccm).

transferred charge during the discharge is high, however, its number of micro-discharge peaks is also higher, which lead to the decrease of average value of the micro-discharge current pulse.

The duration of a single pulse actually depends on the gap distance and the capacitance of the dielectric material, or the amount of charge stored on the dielectric surface [44]. As mentioned above, the average lifetime of micro-discharge current pulses given in figure 11(c) is not the true lifetime of individual micro-discharge channel in the gas gap, and the duration of individual micro-discharge channel during actual discharge is only a few nanoseconds. It can be seen from figure 11(c) that the micro-discharge current pulse duration of the double dielectric reactor with copper mesh electrode is much higher than the duration of the micro-discharge current pulse of the reactor without copper mesh. Combined with the number of micro-discharge peaks given in figure 11(a), it shows that the use of copper mesh as the electrode greatly improves the discharge uniformity in discharge time and space, which is beneficial to the conversion of CO_2.

3.4. Effect of electrode configuration and dielectric material on the optical emission characteristic of DBD plasma

The plasma emission spectra collected during the DBD are also an important source of understanding and analyzing the discharge process. The spectral line distribution of the plasma for different electrode configurations of DBD reactors collected is given in figure 12. It can be seen from figure 12 that the optical emission spectra of the plasma discharge between 300 nm and 850 nm are very informative and contain Fox, Duffendack and Barker (FDB, $A^2\Pi \rightarrow X^2\Pi$) bands of the CO_2^+, (Ångström system, $B^1\Sigma^+ \rightarrow A^1\Pi$ and triplet system, $d^3\Delta \rightarrow a^3\Pi$) bands of excited CO molecules, excited CO_2 molecules (391.2 nm, $^1B_2 \rightarrow X^1\Sigma^+$), excited oxygen molecules (400.5 nm, 406.5 nm), excited O_2^+ (588.3 nm, 602.6 nm), and excited oxygen atom (777.2 nm, 845.0 nm) [45–48]. At a discharge power of 40 W, the Fox, Duffendack and Barker (FDB, FDB, $A^2\Pi \rightarrow X^2\Pi$) bands of CO_2^+ formed by the DBD have the highest emission intensity, while the two characteristic bands of CO have the second highest emission intensity (Ångström system, $B^1\Sigma^+ \rightarrow A^1\Pi$ and triplet system, $d^3\Delta \rightarrow a^3\Pi$), so the emission intensity of these bands can be used for further analysis of the ionization and dissociation processes of CO_2.

As shown in figure 12, the spectral intensity of CO_2^+ is quite high, which is also observed in other experimental studies about CO_2 decomposition by DBD [41, 49]. As reported in [3, 49], the formation of CO_2^+ molecular ions is through the following reaction

$$e + CO_2 \rightarrow e + e + CO_2^+ \tag{8}$$

The cross section of the collision ionization reaction between electrons and CO_2 molecules is relatively large, and the threshold energy of collision ionization is 13.77 eV, which indicates that the process of generating CO_2^+ under the action of high-energy electrons in DBD is relatively important. CO_2^+ ions are usually generated in the electronic excited states $A^2\Pi$ (at 17.31 eV above CO_2 ground state) [50]. When the excited molecular ions $CO_2^+(A^2\Pi)$ are deexcited to the ground state molecular ions $CO_2^+(X^2\Pi)$, the emission band of CO_2^+ is produced. This is the main source of the CO_2^+ characteristic spectral band located between 300 nm and 420 nm observed in figure 12.

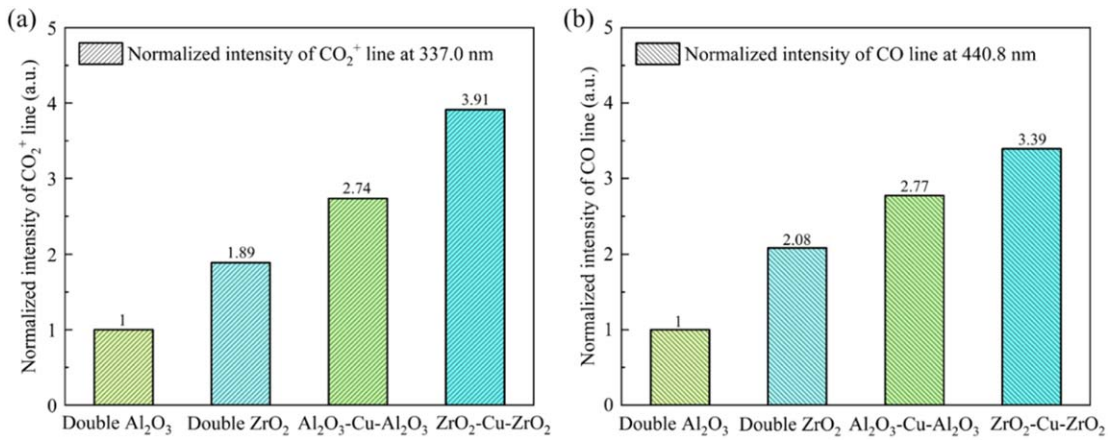

Figure 13. Comparison of normalized spectral line intensity of (a) CO_2^+ and (b) excited CO molecules in different DBD reactors (discharge power of 40 W, CO_2 flow rate of 20 sccm).

Due to the presence of CO_2^+, the accompanying CO_2 dissociation mechanism is dissociative recombination reaction of CO_2^+ as follows

$$e + CO_2^+ \rightarrow CO_2 \rightarrow CO + O \tag{9}$$

This reaction is a highly exothermic process [51]. Since CO_2^+ in a DBD plasma usually appear in the form of electronic excited molecular ions, the products of dissociative recombination reaction are also usually electronic excited CO molecules or excited oxygen atoms.

It can be seen that the the formation of CO_2^+ molecular ions is connected with the release of an electron and while the formation of CO species is connected with the dissociation of CO_2 molecules. Therefore, we extracted two spectral lines from figures 12, 337.0 nm as well as 440.8 nm, for normalized comparison of their emission intensities in the following analysis, as shown in figure 13, for the analysis of the discharge characteristics of the reactors with different electrode configurations.

As can be seen from figure 13, for DBD reactors with different dielectric materials and electrode configurations, the use of dielectrics with higher relative permittivity, and the use of double-dielectric layer with copper mesh electrode all result in enhanced CO_2^+ as well as CO spectral line intensity, which is also a reflection of enhanced discharge efficiency of CO_2 system.

4. Conclusions

In this experimental study, the effect of different electrode configurations, dielectric materials of DBD reactors on CO_2 conversion is investigated. The electrical characteristics, micro-discharge characteristics, and optical emission spectral characteristics of the double dielectric layer reactor with alumina or zirconia as dielectric and the reactor with copper mesh as a high voltage electrode are compared. The results show that both the zirconia reactor with a higher relative dielectric permittivity and the double dielectric reactor with copper mesh electrode are beneficial for improving the CO_2 conversion and energy efficiency.

The analysis of reactors with different electrode configurations further indicates that the use of a reasonable combination of reactors with high relative permittivity as well as reactors with copper mesh electrode can reduce the applied voltage required for reactor discharge, increase the reactor capacitance, and substantially improve the charge transfer capability of the DBD reactor. The analysis of micro-discharge characteristics shows that the double-dielectric reactor with copper mesh as the high-voltage electrode can substantially increase the number of micro-discharge peaks, and improve the uniformity of discharge within the gap to some extent. Optical emission spectra analysis of CO_2 plasma shows that the combination of using high relative permittivity material as well as reactor with copper mesh electrode can effectively improve the discharge efficiency of CO_2.

Acknowledgments

This work was supported by the National Natural Science Foundation of China (Grant Nos. 12175011, 12005010, 11735004) and Open Funding from State Key Laboratory of High-temperature Gas Dynamics, Chinese Academy of Sciences (No. 2021KF08).

Data availability statement

All data that support the findings of this study are included within the article (and any supplementary files).

Conflict of Interest declaration

The authors declare that they have NO affiliations with or involvement in any organization or entity with any financial interest in the subject matter or materials discussed in this manuscript.

ORCID iDs

Hai-Xing Wang https://orcid.org/0000-0001-7426-0946
He-Ji Huang https://orcid.org/0000-0002-1679-4736
Jin-Wen Cao https://orcid.org/0000-0002-1453-5714

References

[1] Kogelschatz U 2003 Dielectric-barrier discharges: their history, discharge physics, and industrial applications *Plasma Chem. Plasma Process.* **23** 1–46
[2] Wagner H E, Brandenburg R, Kozlov K V, Sonnenfeld A, Michel P and Behnke J F 2003 The barrier discharge: basic properties and applications to surface treatment *Vacuum* **71** 417–36
[3] Tu X and Whitehead J C 2012 Plasma-catalytic dry reforming of methane in an atmospheric dielectric barrier discharge: understanding the synergistic effect at low temperature *Appl. Catal. B: Environ.* **125** 439–48
[4] Mei D, Zhu X, Wu C, Ashford B, Williams P T and Tu X 2016 Plasma-photocatalytic conversion of CO_2 at low temperatures: understanding the synergistic effect of plasma-catalysis *Appl. Catal. B: Environ.* **182** 525–32
[5] Bogaerts A, Kozák T, Laer K V and Snoeckx R 2015 Plasma-based conversion of CO_2: current status and future challenges *Faraday Discuss.* **183** 217–32
[6] Chen G, Snyders R and Britun N 2021 CO_2 conversion using catalyst-free and catalyst-assisted plasma-processes: recent progress and understanding *J. CO_2 Util.* **49** 101557
[7] Lebedev Y A and Shakhatov V A 2022 Decomposition of CO_2 in atmospheric-pressure barrier discharge (analytical review) *Plasma Phys. Reports* **48** 693–710
[8] Bogaerts A, Berthelot A, Heijkers S, Kolev S, Snoeckx R, Sun S, Trenchev G, Laer K V and Wang W 2017 CO_2 conversion by plasma technology: insights from modeling the plasma chemistry and plasma reactor design *Plasma Sources Sci. Technol.* **26** 063001
[9] Shao K, Sun S, Meng X, Huang H, Hu Y and Wang H 2022 Experimental study of the effect of argon on the restrike characteristics of nitrogen arc *Plasma Sources Sci. Technol.* **31** 095008
[10] Sun S, Wang H and Bogaerts A 2020 Chemistry reduction of complex CO_2 chemical kinetics: application to a gliding arc plasma *Plasma Sources Sci. Technol.* **29** 025012
[11] Sun S, Wang H, Mei D, Tu X and Bogaerts A 2017 CO_2 conversion in a gliding arc plasma: performance improvement based on chemical reaction modeling *J. CO_2 Util.* **17** 220–34
[12] Cheng J, Wang H and Sun S 2016 Analysis of dissociation mechanism of CO_2 in a micro-hollow cathode discharge *Chinese Phys. Lett.* **33** 108201
[13] Ma T, Wang H, Shi Q, Li S, Sun S and Murphy A B 2019 Experimental study of CO_2 decomposition in a DC micro-slit sustained glow discharge reactor *Plasma Chem. Plasma Process.* **39** 825–44
[14] Kozák T and Bogaerts A 2014 Splitting of CO_2 by vibrational excitation in non-equilibrium plasmas: a reaction kinetics model *Plasma Sources Sci. Technol.* **23** 045004
[15] Aerts R, Martens T and Bogaerts A 2012 Influence of vibrational states on CO_2 splitting by dielectric barrier discharges *J. Phys. Chem.* C **116** 23257–73
[16] Berthelot A and Bogaerts A 2016 Modeling of plasma-based CO_2 conversion: lumping of the vibrational levels *Plasma Sources Sci. Technol.* **25** 045022
[17] Sun S, Kolev S, Wang H and Bogaerts A 2017 Investigations of discharge and post-discharge in a gliding arc: a 3D computational study *Plasma Sources Sci. Technol.* **26** 055017
[18] Sun S, Kolev S, Wang H and Bogaerts A 2017 Coupled gas flow-plasma model for a gliding arc: investigations of the back-breakdown phenomenon and its effect on the gliding arc characteristics *Plasma Sources Sci. Technol.* **26** 015003
[19] Ozkan A, Dufour T, Silva T, Britun N, Snyders R, Bogaerts A and Reniers F 2016 The influence of power and frequency on the filamentary behavior of a flowing DBD—application to the splitting of CO_2 *Plasma Sources Sci. Technol.* **25** 025013
[20] Laer K V and Bogaerts A 2017 Influence of gap size and dielectric constant of the packing material on the plasma behaviour in a packed bed DBD reactor: a fluid modelling study *Plasma Process. Polym.* **14** 1600129
[21] Ozkan A, Dufour T, Bogaerts A and Reniers F 2016 How do the barrier thickness and dielectric material influence the filamentary mode and CO_2 conversion in a flowing DBD? *Plasma Sources Sci. Technol.* **25** 045016
[22] Mei D and Tu X 2017 Conversion of CO_2 in a cylindrical dielectric barrier discharge reactor: effects of plasma processing parameters and reactor design *J. CO_2 Util.* **19** 68–78
[23] Engeling K W, Kruszelnicki J, Kushner M J and Foster J E 2018 Time-resolved evolution of micro-discharges, surface ionization waves and plasma propagation in a two-dimensional packed bed reactor *Plasma Sources Sci. Technol.* **27** 085002
[24] Kruszelnicki J, Engeling K W, Foster J E, Xiong Z and Kushner M J 2017 Propagation of negative electrical discharges through 2-dimensional packed bed reactors *J. Phys. D: Appl. Phys.* **50** 025203
[25] Butterworth T and Allen R W K 2017 Plasma-catalyst interaction studied in a single pellet DBD reactor: dielectric constant effect on plasma dynamics *Plasma Sources Sci. Technol.* **26** 065008

[26] Ding W, Xia M, Shen C, Wang Y, Zhang Z, Tu X and Liu C 2022 Enhanced CO_2 conversion by frosted dielectric surface with ZrO_2 coating in a dielectric barrier discharge reactor *J. CO_2 Util.* **61** 102045
[27] Ray D, Chawdhury P, Bhargavi K V S S, Thatikonda S, Lingaiah N and Subrahmanyam C 2021 Ni and Cu oxide supported γ-Al_2O_3 packed DBD plasma reactor for CO_2 activation *J. CO_2 Util.* **44** 101400
[28] Aerts R, Somers W and Bogaerts A 2015 Carbon dioxide splitting in a dielectric barrier discharge plasma: a combined experimental and computational study *Chem. Sus. Chem* **8** 702–16
[29] Li R, Tang Q, Yin S and Sato T 2007 Investigation of dielectric barrier discharge dependence on permittivity of barrier materials *Appl. Phys. Lett.* **90** 131502
[30] Pipa A V, Koskulics J, Brandenburg R and Hoder T 2012 The simplest equivalent circuit of a pulsed dielectric barrier discharge and the determination of the gas gap charge transfer *Rev. Sci. Instrum.* **83** 115112
[31] Pipa A V, Hoder T, Koskulics J, Schmidt M and Brandenburg R 2012 Experimental determination of dielectric barrier discharge capacitance *Rev. Sci. Instrum.* **83** 075111
[32] Belinger A, Dap S and Naudé N 2022 Influence of the dielectric thickness on the homogeneity of a diffuse dielectric barrier discharge in air *J. Phys. D: Appl. Phys.* **55** 465201
[33] Mei D, Zhu X, He Y L, Yan J D and Tu X 2015 Plasma-assisted conversion of CO_2 in a dielectric barrier discharge reactor: understanding the effect of packing materials *Plasma Sources Sci. Technol.* **24** 015011
[34] Gadkari S and Gu S 2018 Influence of catalyst packing configuration on the discharge characteristics of dielectric barrier discharge reactors: a numerical investigation *Phys. Plasmas* **25** 063513
[35] Francke K P, Rudolph R and Miessner H 2003 Design and operating characteristics of a simple and reliable DBD reactor for use with atmospheric air *Plasma Chem. Plasma Process.* **23** 47–57
[36] Tu X, Gallon H J, Twigg M V, Gorry P A and Whitehead J C 2011 Dry reforming of methane over a Ni/Al_2O_3 catalyst in a coaxial dielectric barrier discharge reactor *J. Phys. D: Appl. Phys.* **44** 274007
[37] Brandenburg R 2017 Dielectric barrier discharges: progress on plasma sources and on the understanding of regimes and single filaments *Plasma Sources Sci. Technol.* **26** 053001
[38] Peeters F J J and Sanden M C M V D 2015 The influence of partial surface discharging on the electrical characterization of DBDs *Plasma Sources Sci. Technol.* **24** 015016
[39] Butterworth T, Elder R and Allen R 2016 Effects of particle size on CO_2 reduction and discharge characteristics in a packed bed plasma reactor *Chem. Eng. J.* **293** 55–67
[40] Reichen P, Sonnenfeld A and Rohr P R V 2011 Discharge expansion in barrier discharge arrangements at low applied voltages *Plasma Sources Sci. Technol.* **20** 055015
[41] Brehmer F, Welzel S, Sanden M C M V D and Engeln R 2014 CO and byproduct formation during CO_2 reduction in dielectric barrier discharges *J. Appl. Phys.* **116** 123303
[42] Gibalov V I and Pietsch G J 2000 The development of dielectric barrier discharges in gas gaps and on surfaces *J. Phys. D: Appl. Phys.* **33** 2618–36
[43] Ma Y, Wang Y, Harding J and Tu X 2021 Plasma-enhanced N_2 fixation in a dielectric barrier discharge reactor: effect of packing materials *Plasma Sources Sci. Technol.* **30** 105002
[44] Kogelschatz U 2010 Collective phenomena in volume and surface barrier discharges *J. Phys. Conf. Ser.* **257** 012015
[45] McCallum J C and Nicholls R W 1972 Relative intensity measurements on the fox-duffendack-barker ($A^2\Pi_u$-$X^2\Pi_g$) and the ultraviolet doublet ($B^2\Sigma_u^+$-$X^2\Pi_g$) band systems of CO_2^+ *J. Phys. B: Atom. Molec. Phys.* **5** 1417–26
[46] Silva T, Britun N and Godfroid T 2017 Understanding CO_2 decomposition in microwave plasma by means of optical diagnostics *Plasma Process. Polym.* **14** 1600103
[47] Bartnik A, Skrzeczanowski W, Wachulak P, Fok T, Wegrzynski Ł, Szczurek M and Fiedorowicz H 2021 Spectral investigations of low-temperature plasma induced in CO_2 gas by nanosecond pulses of extreme ultraviolet (EUV) *Plasma Sources Sci. Technol.* **30** 115008
[48] Du Y, Tamura K, Moore S, Peng Z, Nozaki T and Bruggeman P J 2017 CO($B^1\Sigma^+ \rightarrow A^1\Pi$) angstrom system for gas temperature measurements in CO_2 containing plasmas *Plasma Chem. Plasma Process.* **37** 29–41
[49] Xu S, Whitehead J C and Martin P A 2017 CO_2 conversion in a non-thermal, barium titanate packed bed plasma reactor: the effect of dilution by Ar and N_2 *Chem. Eng. J.* **327** 764–73
[50] McConkey J W, Burns D J and Woolsey J M 1968 Absolute cross sections for ionization and excitation of CO_2 by electron impact *J. Phys. B: Atom. Mol. Phys.* **1** 71–6
[51] Fox J L 2005 Effects of dissociative recombination on the composition of planetary atmospheres *J. Phys. Conf. Ser.* **4** 32–7